Journal of Hydrology: Regional Studies 59 (2025) 102456

Contents lists available at ScienceDirect

Journal of Hydrology: Regional Studies

journal homepage: www.elsevier.com/locate/ejrh

Topographic indices and ERA5-Land data to describe soil moisture variability in a Central European beech forest

Marian Schönauer [a], Stephen B. Asabere [b], Daniela Sauer [b], Simon Drollinger [b,c,*]

[a] Department of Forest Protection and Wildlife Management, Faculty of Forestry and Wood Technology, Mendel University in Brno, Brno, Czech Republic
[b] Department of Physical Geography, University of Göttingen, Göttingen, Germany
[c] Bioclimatology, University of Göttingen, Göttingen, Germany

ARTICLE INFO

Keywords:
Spatio-temporal variability
Topographic modelling
Beech forest
Climate change
Ecosystem functioning
Forest management
Soil water content

ABSTRACT

Study region: Temperate beech forest in central Germany's low mountain range
Study focus: Soil moisture is essential for ecosystem functioning, influencing hydrological, biological, and biogeochemical processes. It regulates water, energy, and carbon cycles, supporting ecosystem organization, biodiversity, and vegetation resilience. However, climate change and human activities increasingly disrupt soil moisture dynamics, altering spatio-temporal variability due to altered precipitation, rising temperatures, and droughts, making prediction attempts a challenge. This study examines a temperate beech forest in central Germany's low mountain range, aiming to: (1) analyse spatio-temporal variations in soil moisture and temperature, (2) assess correlations with topographic indices across seasons, and (3) validate ERA5-Land retrievals. We employed 62 automatic sensors and manual measurements at 236 sites within a 900 × 600 m area. Field data were merged with ERA5-Land reanalysis and topographic indices, including depth-to-water and topographic position indices, to assess their performance in predicting soil water content spatial patterns.
New hydrological insights for the region: Temporal variation exceeded spatial variation by 3.60–3.68 times. While soil moisture was associated with mesorelief (topographic position index), the correlation was weak. Flow accumulation-based indices were ineffective in capturing spatial soil moisture variation and failed to model spatio-temporal variability. This suggests that model results need to be reconsidered, and suitable indices developed. Insights from this study contribute to improving soil–vegetation–atmosphere models and support sustainable forest management in a changing climate.

1. Introduction

Soil moisture is the amount of water held in the soil pores in active unsaturated soil layers. It is a key state variable of land ecosystems that reflect interactions between water, energy, and carbon cycles (Berg and Sheffield, 2018; Green et al., 2019) and can be quantified as soil water content (SWC). As a critical interface between the atmosphere, vegetation, and subsurface, soil moisture regulates land-surface interactions and drives hydrological, biological, and biogeochemical processes in forest ecosystems (Rahmati et al., 2024; S.U. et al., 2014; Vereecken et al., 2022). It influences water and energy exchange, plays a major role for plant growth and

* Corresponding author at: Department of Physical Geography, University of Göttingen, Göttingen, Germany.
E-mail address: simon.drollinger@uni-goettingen.de (S. Drollinger).

https://doi.org/10.1016/j.ejrh.2025.102456
Received 16 February 2025; Received in revised form 6 May 2025; Accepted 7 May 2025
Available online 13 May 2025
2214-5818/© 2025 The Author(s). Published by Elsevier B.V. This is an open access article under the CC BY license (http://creativecommons.org/licenses/by/4.0/).

understory microclimate, ecosystem organization and biodiversity (Greiser et al., 2024; Vereecken et al., 2014), litter decomposition, microbial soil CO_2 production and ultimately weathering and soil carbon sequestration and soil formation (Drollinger et al., 2025; Fowler et al., 2021; Pendergrass et al., 2017). Thus, analysing small-scale spatial and temporal dynamics of SWC is of utmost importance for improving our understanding of ecosystem functioning and improve prediction models.

Anthropogenic warming intensifies daily rainfall but reduces its frequency, leading to larger rain events and prolonged dry spells (Konapala et al., 2020; Wood and Ludwig, 2020). These shifts have complex, sometimes opposing effects on plant photosynthesis and growth, complicating predictions for the carbon cycle. Contrasting responses in dry and wet ecosystems arise from nonlinear plant reactions to SWC, driven by various ecohydrological mechanisms (Feldman et al., 2024). Recent studies suggest that increasing ecosystem vulnerability due to decreasing SWC could further reduce vegetation carbon uptake under intensified droughts, thereby exacerbating climate change (Li et al., 2022). Climate and societal changes are projected to further exacerbate water scarcity in many regions worldwide in the coming decades, emphasizing the need to develop general decision-making framework to enhance policy-making (Greve et al., 2018). To implement such decision support systems, realistic future projections and indicators of SWC are required, derived by models that are based on measured values.

Climate change affects transpiration, evaporation, and precipitation, influencing green and atmospheric water availability and necessitating resilient ecosystems and adaptive water management policies (Te Wierik et al., 2020). However, such adaptations can only be implemented when an understanding and accurate quantification of spatio-temporal variation in SWC is guaranteed. Given the limited spatial and temporal scope of in-situ data and the high variability of SWC contents across scales (Vereecken et al., 2014), model-based representations of SWC can be useful for improving projection accuracy. Although a precise representation of SWC variations remains a critical challenge, detailed insights are needed to improve modelling, prediction, and management of green water availability and scarcity (Liang et al., 2020; Schyns et al., 2015). Projections often suggest that anthropogenic climate change will lead to heightened drought conditions due to increased evaporative demand (Vicente-Serrano et al., 2020). However, discrepancies between projections and observed trends suggest that increased evaporative demand initially raises evapotranspiration and depletes SWC, while extreme water deficits cause vegetation to experience water limitations, ultimately reducing evapotranspiration (Berg and Sheffield, 2018). Given these challenges, precise modelling of SWC becomes not just a scientific pursuit but a necessity for sustainable ecosystem management.

Modelling techniques to adequately represent SWC dynamics across space and time have been developed since decades. This involved studying SWC dynamics using models to interpret observed SWC variability (Chen et al., 2017; Vereecken et al., 2014; Western and Blöschl, 1999), to assess the relative importance of controlling factors, such as saturated hydraulic conductivity (De Oliveira et al., 2021; Martinez et al., 2013; Zhou et al., 2021), or to derive statistical distributions of soil parameters (Cosby et al., 1984; Scharnagl et al., 2011; Vereecken et al., 2022). The spatio-temporal distribution of SWC is influenced by local factors, such as vertically dominant fluxes governed by soil hydraulic properties and vegetation, and non-local factors, including climate variability and lateral processes driven by topography (Grayson et al., 1997). Beven and Kirkby (1979) related a hydrological model based on the effects of a channel network topology and contributing areas on SWC variations. Sørensen et al. (2006) further developed such models and validated them through in-situ campaigns. One of the more recently developed and tested methods is called 'depth-to-water' (DTW) (Murphy et al., 2011, 2007), which uses a channel network of simulated water flows and calculates the vertical distances to the nearest channels. DTW was validated extensively in Fenno-Scandinavian countries, and found to perform relatively well in predicting wet areas compared to other indices (Ågren et al., 2014; Larson et al., 2022). In recent years, machine learning algorithms have advanced SWC prediction. These developments include the use of downscaling techniques to refine coarse remote sensing data (Liu et al., 2020; Nguyen et al., 2022; O. and Orth, 2021; Peng et al., 2021), as well as various topographic indices calculated from digital elevation models (DEMs). Ågren et al. (2021) used 28 topographic predictor variables in a machine learning library to predict SWC across the entire Swedish forest landscape at a 2 m resolution. Although topographic modelling approaches are widely used, they often fail to adjust for seasonal changes in soil water regimes. Models combining spatial with temporal components enable raster predictions for any specified time and location (Nketia et al., 2022). Schönauer et al. (2022, 2024) conceived and tested a downscaling approach to create a spatio-temporal SWC model. For this, high-resolution but static topographic maps (1×1 m) were combined with temporal SWC data of coarse spatial resolution (9×9 km) to achieve high accuracies. A key source for such data is the European Centre for Medium-Range Weather Forecasts (ECMWF), operator of the Copernicus Climate Change Service, and its ERA5-Land dataset (Copernicus Climate Change Service, 2019; Muñoz-Sabater et al., 2021). Moreover, recent developments by the Finnish Meteorological Institute (2023) point towards integrating medium- and long-range weather forecasts used for SWC predictions and their practical applications. These advancements address the gaps in seasonal SWC predictions and can enhance practical decision-making, e.g. by knowing *where* and *when* soils are wet and therefore sensitive to traffic-induced damages (Hoffmann et al., 2022; Latterini et al., 2024), relating vegetation characteristics to SWC regimes (Bartels et al., 2018), influence of complex terrain on vegetation–climate–topography relationships (Adams et al., 2014), or the strategic planting of drought-resistant species in selected areas.

Although variations in SWC and the spatial distributions of wetlands and their relationship to topographic information have been studied in boreal landscapes, knowledge of the relationship between SWC and topographic indices is limited for Central Europe. Numerous modelling exercises depict SWC as a result of topographic differences without empirical evidence of these relationships for specific areas. This is especially true for more complex landscapes with varying slope gradients and positions, vegetation and soil properties. To provide additional evidence on the relationship between SWC and landscape indices and enhance the understanding of SWC variability in deciduous forests of Central Europe, we launched a measuring campaign, capturing SWC and soil temperature in a 900×600 m sized experiment, and compared the captured data with static but fine scaled (1 – 20 m resolution) topographic indices and coarse scaled (9×9 km) but temporal ERA5-Land data. In particular, the research objectives were to:

1. determine variation of SWC and temperature in a temperate deciduous forest and compare it in a space-time continuum
2. quantify correlations between observed soil water content and topographic indices, considering seasonally changing conditions
3. validate the quality of ERA5-Land retrievals in capturing temporal variability in SWC and soil temperature

2. Material and methods

2.1. Study area

The study area is located in a central German upland region (51.5665°N, 10.0808°E; 280 m asl; Fig. 1). The main tree stock consists of ~100-year-old European beech trees (*Fagus sylvatica* L.), mixed with approximately 5 % European larch (*Larix decidua* Mill.), at a stocking level of 80 – 90 %. Mean annual precipitation is 738 ± 132 mm and mean annual air temperature is 9.4 ± 0.74°C (1991 – 2020; local weather station data Ebergötzen). Forest soils in the study area have developed on Lower Triassic sandstone (*Bundsandstein*), overlain by Pleistocene periglacial slope deposits. In large parts of the study area, these soils have developed into *Cambisols*, characterized by active clay migration, acidification, and, in some areas, early-stage podsolization. Soil particles are dominated by 73 % sand, 23 % silt and 4 % clay (Diederichs, 2018). A distinctive feature of the area is the Holocene colluvium, which can be found on the lower valley slopes.

2.2. In-situ data

2.2.1. Precipitation

Gross precipitation (P [mm]) was measured at the nearest open area on an adjacent meadow in the east of the study area using the precipitation gauge Pluvio² S (Ott Hydromet GmbH, Kempen, Germany) with a collecting area covering 200 cm^2, a resolution of 0.001 mm and an accuracy of ± 0.1 mm. Data from 2021 to 11–30 to 2022–12–01 was used for this analysis. It must be considered that net precipitation reaching the forest ground does not correspond to the gross precipitation but is determined by varying throughfall fractions, depending on rainfall patterns and canopy coverage (Drollinger et al., 2025).

2.2.2. Soil water content and soil temperature

Manual measurements of soil water content (SWC [%v/v]) were conducted using a handheld moisture meter (HH-2 Field, Delta-T devices, Cambridge, UK; impedance measuring technique). The measurements involved inserting 75 mm long rods vertically into the soil after removing coarse litter. This time-series measurement approach involved 11 repetitions conducted between November 2021 and December 2022, at approximately one-month intervals across 236 measurement sites. All these sites were located within a 900 × 600 m experimental area, with site-to-site spacing ranging from 25 m to 100 m (Fig. 1). A narrower spacing was chosen in the valley regions, where SWC was anticipated to be higher compared to the flat or elevated areas of the experiment. Due to the temporal characteristics of this dataset, it is referred to as 'monthly' in this study. Additionally, within the experimental area, 62 TMS-4 Standard

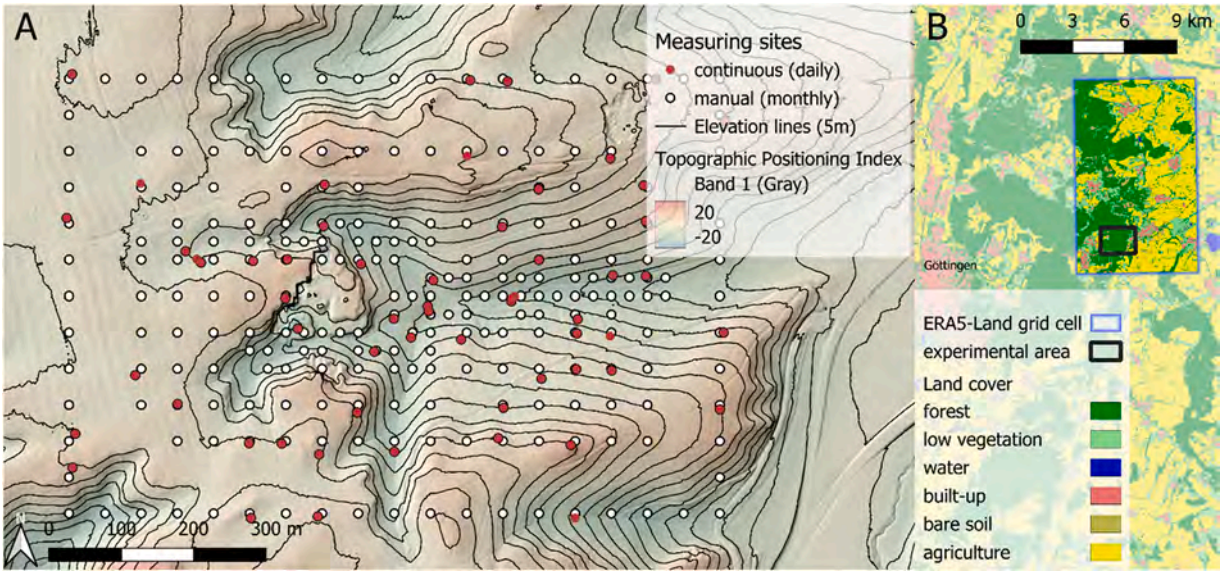

Fig. 1. (A) Overview of the study area in a beech forest stand in central Germany (51.5665°N, 10.0808°E). Red dots represent locations of the 62 automatic SWC and temperature loggers, white dots represent the 236 manual measurement sites, where SWC and temperature was measured monthly. Colours indicate Topographic Positioning Index. (B) shows the land cover classification and the respective grid cell of ERA5-Land (details given below).

sensors (TOMST s.r.o., Czech Republic; Wild et al., 2019) were installed. These sensors captured both SWC and soil temperature (ST [°C]) at a soil depth of −6 cm from 2022-01–01 to 2022–10–25. To determine SWC, the raw moisture signal of the sensors (SMcount) had to be converted into SWC using Eq. (1), calculated for the given soil class, according to TOMST s.r.o. (n.d.):

$$\mathbf{SWC} = \left(-\mathbf{1.55397} \times \mathbf{10^{-8}} \times \mathbf{SMcount^2} + \mathbf{0.00024989} \times \mathbf{SMcount} - \mathbf{0.158953548}\right) \times \mathbf{100} \quad (1)$$

The time-series of SWC originating from installed sensors underwent visual assessment to ensure the integrity of the data. If clear indications suggested that the data was unreliable – such as a distinct and abrupt drop in the SWC readings from one sensor while others remained stable – it was flagged as a potential issue, possibly caused by events like sensor displacement due to animal activity. Accordingly, phases with highly improbable values were excluded from the analysis. Additionally, some sensors were placed as pseudo-replicates at distances of less than 1 m, necessitating their removal. Consequently, the initial dataset of 1.77×10^6 observations was reduced to 1.43×10^6 observations, and the number of sensors used in this analysis decreased from 62 to 53. These 53 sensors additionally measured the air temperature at a height of 15 cm.

2.3. Topographic indices

To calculate the topographic indices, we utilized a digital elevation model (DEM) with 1 m a resolution provided by the Lower Saxony State of Germany. We employed the R programming language (version 4.3.0, R Core Team, 2023) and RStudio (Posit PBC, Massachusetts, USA) along with the "rgrass" package (Bivand et al., 2023) to utilize GRASS (Awaida and Westervelt, 2020) commands in the R interface. The GRASS-command 'r.hydrodem' was used to remove all sinks from the DEM.

2.3.1. Depth-to-water

Subsequently, we computed depth-to-water (DTW [m]) maps using the DTW concept, as conceived and developed by Fan-Rui Meng, Jae Ogilvie and Paul Arp, following the script by Schönauer and Maack, (2021). The DTW maps were generated using flow initiation areas (FIA) of varying sizes (0.25 ha, 1.00 ha, 2.00 ha and 4.00 ha). The DTW maps were labelled DTW0.25, DTW1, DTW2, and DTW4, respectively, corresponding to the FIA used. A smaller FIA resulted in a DTW map for wetter conditions, while a larger FIA represented drier conditions. For more detailed information, refer to Murphy et al. (2009), (2011).

2.3.2. Topographic position index

The topographic position index (TPI [m]) compares the elevation of each cell to its neighboring cells, where positive values indicate hills or ridges, and negative values indicate valleys or depressions. TPI was calculated using the 'spatialEco' package (Evans and Murphy, 2023) considering rectangular moving windows with side lengths of 50, 100, or 200 m.

2.3.3. Topographic indices based on different resolution

The topographic wetness index (TWI, Sørensen et al., 2006) characterizes the runoff behavior of each cell within a DEM and is regarded as an indicator of relief-induced SWC. Recognizing that TWI's performance is influenced by scale (Ågren et al., 2014; Larson et al., 2022), we resampled the DEM into coarser grids through aggregation. This yielded DEMs with resolutions of 1, 5, 10, 15, and 20 m. For each of these DEMs, we computed TWI (using the GRASS command 'r.watershed'), flow accumulation (FlAc [m^2], using 'r.watershed'), and terrain slope (Slope [%], using 'r.slope.aspect').

In prior work, we evaluated the quality of each topographic index and its variations (e.g., TPI50, TPI100, and TPI200) in predicting spatial patterns of SWC. Linear models and the coefficient of determination R^2 were employed for this assessment, calculated for selected days and the full spatial extent (compare to Fig. 4). To mitigate issues of collinearity, only the best-performing configurations of these indices were considered for subsequent analysis (e.g., TPI200 for both SWC and soil temperature).

2.4. ERA5-Land data

To generate time series of ERA5-Land reanalysis data, we used the package "ecmwfr" (Hufkens et al., 2019) to download hourly raster files of the variables 'Volumentric soil water layer [1–4]' and 'Soil temperature level [1–4]' from the Copernicus Climate Change Service (2019), covering the time span of field observations. Subsequently, rasters of each of the eight variables were stacked to extract the values of the nearest grid cell for each site. The entire experimental area was covered by a single ERA5-Land grid cell, resulting in identical values across all measurement positions at any given time (Fig. 1). The land use within this grid cell was predominantly agricultural land and forest (39 % and 38 %, respectively), with smaller proportions of low vegetation (4 %) and built-up infrastructure (3 %), based on a land cover classification map (mundialis GmbH & Co. KG, 2025).

The extracted values were labelled with date and measuring site. Then mean values of in-situ SWC data were merged with retrievals obtained from ERA5-Land data, considering four different soil depths referred to as 'Layers' for SWC or 'Levels' for soil temperature (Layer/Level 1: 0–7 cm, 2: 7–28 cm, 3: 28–100 cm and 4: 100–289 cm).

2.5. Data fusion and analysis

Given the data's varying temporal resolution ranging from 15-minute intervals (for SWC and ST) to hourly intervals (for ERA5-Land) and even monthly measurements we opted to aggregate the data into daily means. Therefore, daily values were extracted for

the days of the monthly measuring campaigns and added to the monthly data. This was done to increase spatial granularity, as the number of observations per month increased from 236 to 289 at nine months. The next step involved merging the data by site and date, followed by analysis using R and RStudio (details given in 2.3). Subsequently, mean values of SWC and ST were computed for each day across all sites. To assess the variation in soil water content and temperature on the temporal and spatial scale, we created variograms and performed Levene's Tests to compare the variance on each scale. Mean values of in-situ SWC and ST were then compared to ERA5-Land values. Since we anticipated varying performance depending on the Layer or Level of the ERA5-Land estimates used, we included all available Layers and Levels in the comparison with in-situ values, which would naturally correspond to Layer/Level 1. Linear correlations were established for each day, examining the relationships between SWC or ST and the selected variations of topographic indices. Separate analyses were conducted for monthly and daily SWC data. To assess the quality of the fitted models, we utilized root mean square error (RMSE), Pearson coefficient of correlation (r), bias, and coefficient of determination (R^2), as needed for their respective purposes. A significance level of $\alpha = 0.05$ was adopted for all tests. The reported values are presented as mean ± standard deviation.

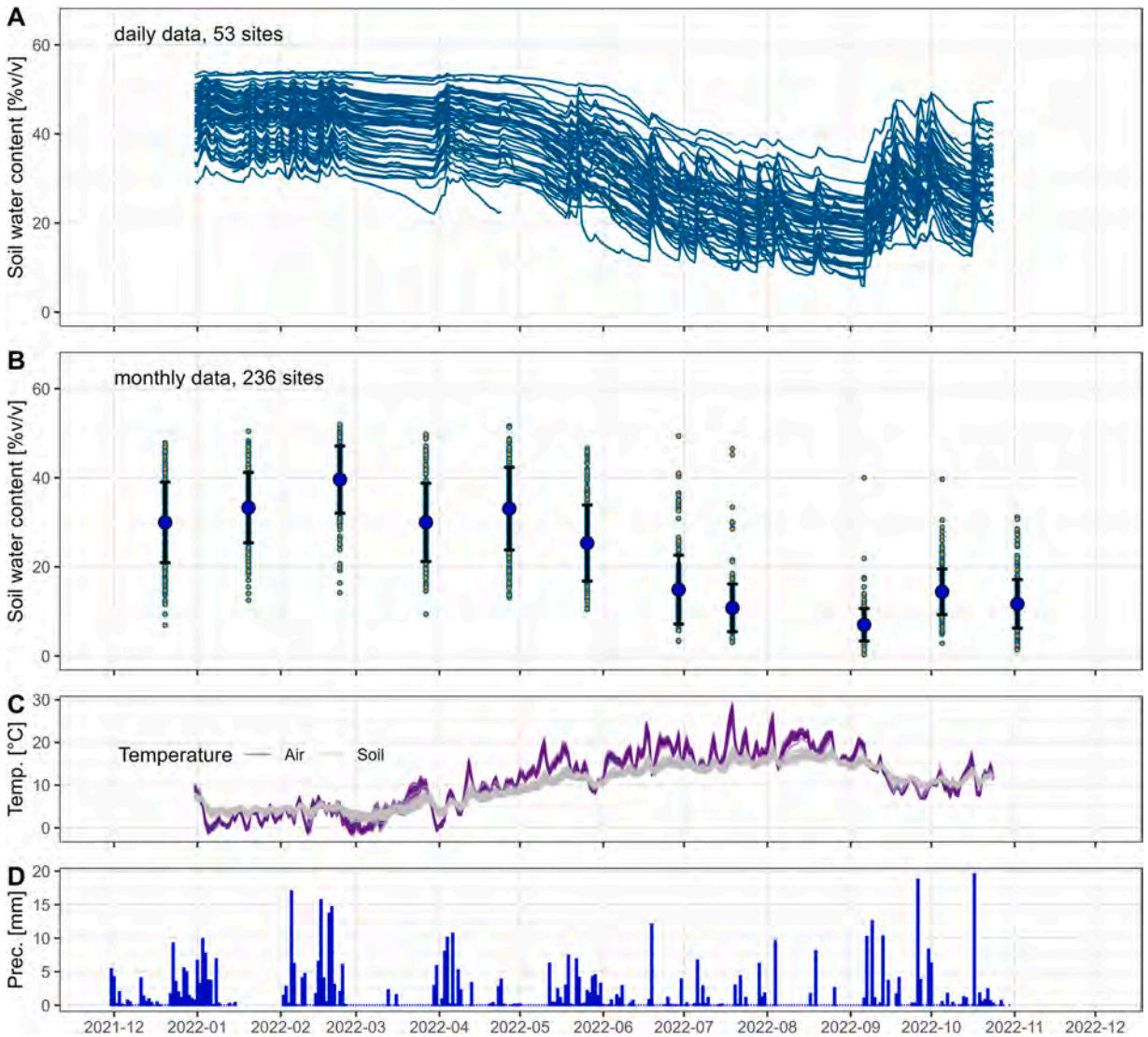

Fig. 2. Soil water content was measured continuously on 53 sites (A), and monthly at 236 sites (B, individual values, mean values and standard deviation) within a 900 × 600 m experiment in a forest stand of *Fagus sylvatica*, located in central Germany. Continuous measurements of soil water content, soil temperature (C, grey lines), and above-ground temperature (C, purple lines) were obtained using TMS-4 Standard sensors. Additionally, precipitation data were collected from an automatic gauge situated on an adjacent meadow, 110 m to the east of the experimental area.

3. Results

3.1. In-situ soil water content, temperature, and precipitation

The overall trend showed a good agreement between the two measurement methods (Fig. 2A&B). However, during the summer drought period in 2022 (June to September 2022), the monthly measurements of the 236 sites averaged 10.90 ± 6.65 % v/v, indicating significantly drier (*t*-test, $p < 0.001$) conditions compared to 24.37 ± 7.77 % v/v of the daily measurements. The minimum SWC within the monthly data occurred on September 7th, with an average value of 7.01 ± 3.66 % v/v. Driest conditions within the daily data were recorded on the same day, with a mean value of 17.7 ± 5.85 % v/v. Differences between the highest daily or monthly means occurred at a lower magnitude. The highest mean value within the monthly data occurred on February 24th, averaging at 39.6 ± 7.54 % v/v. The highest values within the daily data were observed on January 5th, with 46.1 ± 4.86 % v/v.

During the year of observation, the total precipitation recorded at the sites was 548 mm, with 287 mm captured between April and October (Fig. 2D). The highest daily rainfall occurred on October 18th, with an amount of 20.3 mm. On days with precipitation, the average rainfall intensity was 2.89 ± 3.58 mm.

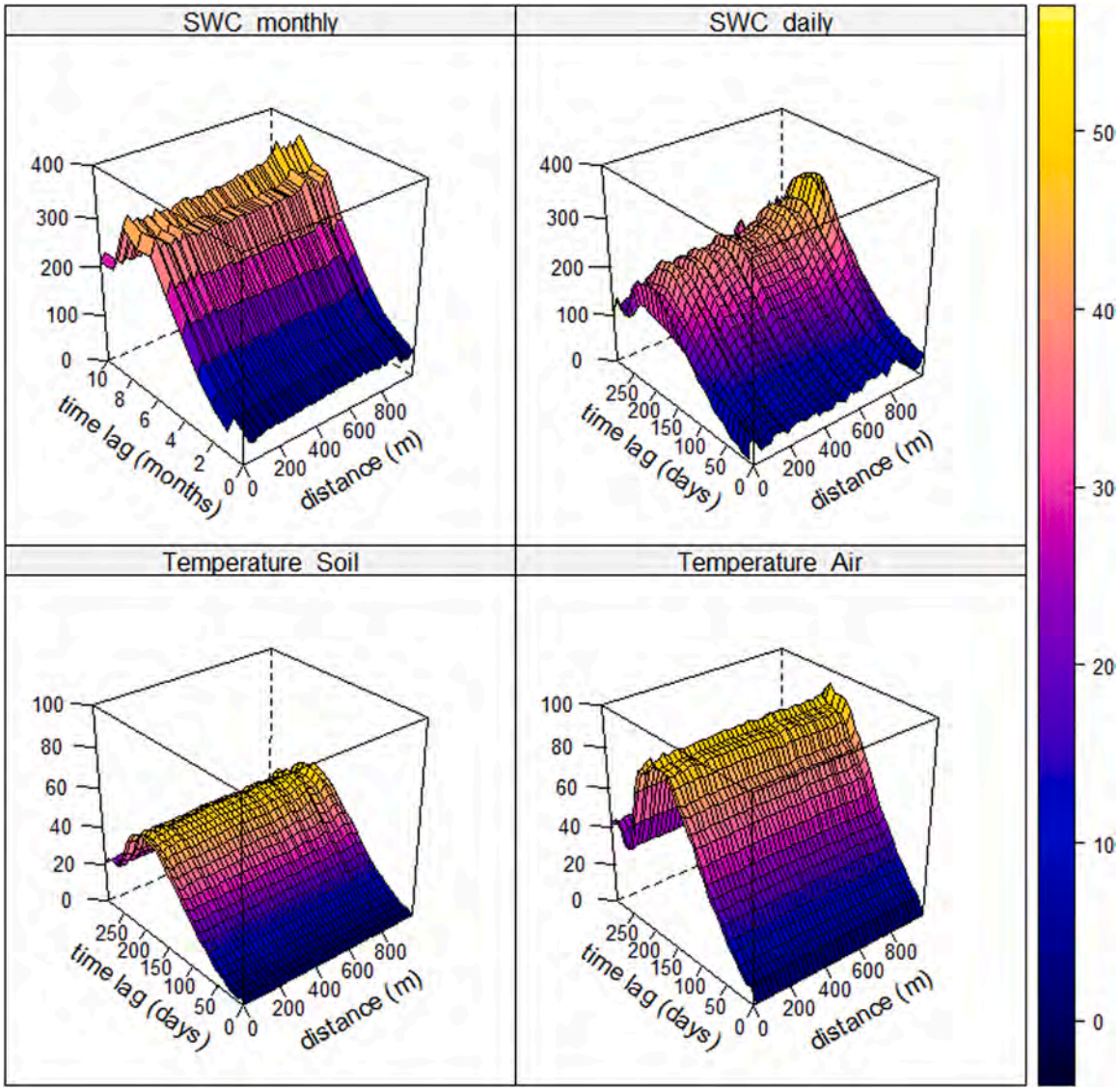

Fig. 3. Variograms show the spatiotemporal dependence of a soil water content and temperature by illustrating how variance (on Z-axis, 0–400) changes with increasing distance between sample points and increasing time lag between measurements. Two data sets were analysed: monthly measurements done with a handheld moisture meter at 236 sites and continuous (daily) measurements by TOMST data loggers at 53 sites. Mind different scales along the Z-axis.

The air temperature near the surface exhibited seasonal variations (Fig. 2C). During the winter months (January to February), the average air temperature was 2.94 ± 2.27 °C. The temperature gradually increased and reached its peak on July 20th, with a maximum of 27.3 ± 0.89 °C. Soil temperature closely followed the pattern of air temperature (Fig. 2B), although with smaller fluctuations. The highest soil temperature was recorded in August, with an average of 17.6 ± 0.68 °C.

3.2. Spatio-temporal variations of soil water content and temperature

Variograms are used to depict variations in soil water content (Fig. 3). SWC from both origins (monthly and daily) showed a strong dependence on time lag. Overall, the variance over time averaged 126 and 81 for the monthly and daily data, respectively. The distance-dependent variance was substantially smaller (Levene's Test, $p < 0.001$), averaging at 35 or 22, respectively. Similar patterns were observed for soil and air temperatures, with significantly lower variance along the spatial scale as compared to the temporal one (Levene's Test, $p < 0.001$, Fig. 3).

3.3. Spatial patterns of soil water content and temperature

To ascertain the interrelations between SWC values and topographic indices, we populated the monthly data with the daily ones. By fitting linear models between SWC and diverse topographic indices, we obtained Pearson's r values for each measurement day and topographic index (Fig. 4). During wet conditions from January to April (Fig. 2A&B), the DTW for moist scenario (DTW0.25) was positively associated with SWC. Similar observations were made for DTW1 and DTW4. However, positive correlations were not plausible, as low values of DTW typically indicate moist soil, contrary to what our data indicated. We barely could detect any association between measured SWC values and the topographic DTW index. The only significant correlation occurred in July but lacked explanatory power to account for the variation of soil water content ($R^2 = 0.0106$).

Flow accumulation (FlAc15) revealed weak positive correlations with SWC. Significant associations were observed in June and

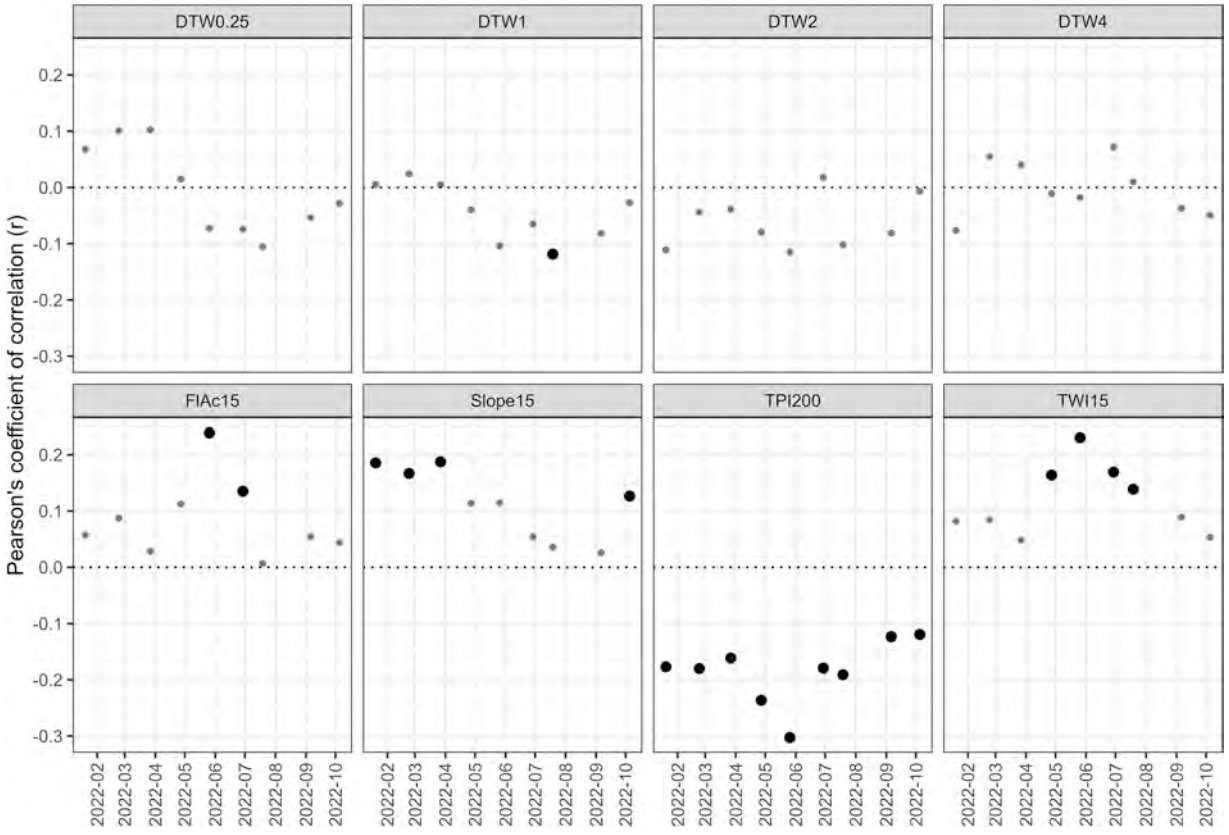

Fig. 4. Pearson coefficient of correlation between soil water content (SWC, n = 298, one measurement per month) and topographic indices, for each month during the study period. SWC was measured manually (236 sites) and with TMS-4 sensors (53 sites) in a 900 × 600 m experiment within a broad-leaved stand in Germany. Linear models were fitted between in-situ measurements and topographic indices, including depth-to-water (DTW), flow accumulation (FlAc), terrain Slope, topographic position index (TPI), and topographic wetness index (TWI), with different flow initiation areas or ground resolutions of the digital elevation model as indicated by the numeric pattern. Points represent the resulting Pearson coefficients of correlation (r). Significant correlations ($p < 0.05$) are shown in bold.

July, when soils were drying out (Fig. 2A&B). Similar findings were observed for the topographic wetness index (TWI15). In contrast to the strongest correlations during summer for the indices FlAc15 and TWI15, terrain Slope15 revealed significant but weak correlations during moist conditions, from January to March, and in October.

Compared to the above-mentioned topographic indices, the terrain position index, calculated with a focal width of 200 × 200 m (TPI200) performed best. The negative correlation coefficients indicate that SWC was higher at depressions, and lower on ridges. Correlations between SWC and TPI200 were always significant, with an overall R^2 of 0.013. In May 2022, R^2 peaked, explaining 9 % of the SWCs variation.

3.4. Interrelation between in-situ measurements and ERA5-Land retrievals

Given the limited value that topographic indices provided in the spatial prediction of SWC or ST, we opted to proceed with analyzing daily mean values from the continuously measuring TMS-4 sensors. These mean values were compared to ERA5-Land retrievals, incorporating the different depths of Layers and Levels. The RMSE was calculated by comparing in-situ SWC values with SWC_{ERA} for each Layer (Fig. 5A). The lowest RMSE was achieved when SWC was compared to SWC_{ERA} Layer 1 (5.7 % v/v, daily data), indicating a strong agreement between the measurements and the estimates. This might be due to a direct correspondence between the measurement depths and the prediction for Layer 1. A bias of −2.4 % v/v means that the SWC_{ERA} Layer 1 was slightly underestimating the true soil water content on average. The strongest correlation, however, was observed between SWC and SWC_{ERA} Layer 3, with an R^2 of 0.91 (0.87 for the monthly data). Using this Layer, there was a stronger dry bias of −5.7 %v/v. To address this bias, a post-measurement correction was applied. The absolute value of the bias was added as constant term to the values of SWC_{ERA} Layer 3, shown as a dashed line in Fig. 5a. Through this correction, the RMSE was reduced to 2.7 %v/v, while maintaining the high R^2 of 0.91 for the daily dataset.

The ERA5-Land retrievals of soil temperature (ST_{ERA}) demonstrated a high suitability in simulating actual soil temperature ST (Fig. 5B). The RMSE values were consistently low, reaching 1.8 °C when comparing ST to ST_{ERA} Level 3, resulting in an R^2 of 0.95. When considering ST_{ERA} Level 2 as an independent variable, the correlation yielded an even higher R^2 of 0.98, although the RMSE

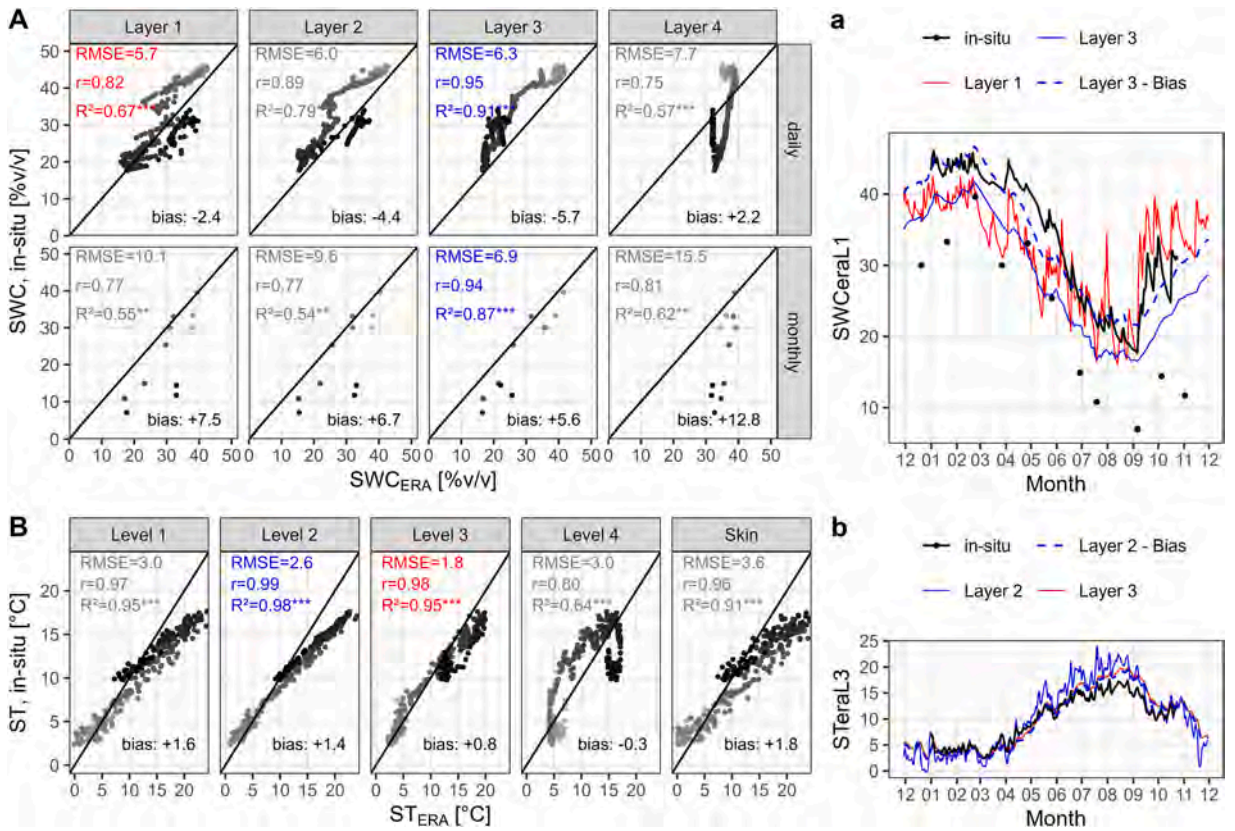

Fig. 5. Daily measurements of soil water content (SWC, A) and soil temperature (ST, B) were collected in a deciduous forest stand on a *Cambisol* in Germany, from December 2021–2022. The in-situ values were compared to ERA5-Land retrievals from different Layers/Levels. Root mean square error (RMSE), Pearson coefficient of correlation (r), coefficient of determination (R^2), and bias were calculated for each comparison. Comparisons with the lowest RMSE are indicated in red, while those with the highest R^2 are highlighted in blue. The time series of SWC is depicted in (a), and the bias of Layer 3-values was added as a dashed blue line. The time series of ST is shown in (b), where the values of Level 2 were modified by correcting the systematic deviations from measured values.

increased slightly to 2.6 °C. Notably, the beta coefficient of the correlation between ST and ST_{ERA} Level 2 was found to be lower than 1. To address this, we employed a linear model, using the beta coefficient and intercept, to predict values of ST based on ST_{ERA} Level 2. The resultant comparison between ST and the predicted ST_{ERA} values exhibited a remarkably low RMSE of 0.6°C, with a high R^2 of 0.98 (shown as the dashed line in Fig. 5b).

4. Discussion

The temporal dynamics of SWC whether captured through continuously measuring sensors at 53 sites or based on manual monthly measurements at 236 sites were generally in agreement between the measurement approaches (Fig. 2). Differences occurred mainly during drought period from June to September 2022. For this time, manual measurements revealed lower magnitudes relative to automatic measurements. This difference can be attributed to the spatial distribution of the sensors as compared to the manual measurements. While the manual measurements were systematically distributed across the 900 × 600 m experiment, yet with higher density in the valley, the majority of automatic sensors was positioned within the valley (central area in Fig. 1). This is in line with the correlations observed between SWC and the topographic indices TPI200. The topographic positioning index TPI, calculated with a focal width of 200 m, gives a robust representation of the mesorelief, and thereby reflects the mentioned valley (Fig. 1).

TPI200 proved to be the topographic predictor with the best scoring, based on the consistently negative and significant correlation coefficients (Fig. 4). The remaining topographic indices performed poor. TWI revealed significant responses with SWC only from April to July, when soils were drying out. This index is based on slope and upstream contributing area. Both Slope and FlAc (which can be seen as upstream contributing area) showed significant correlations with SWC, but only in selected months. It can be deduced that the flow accumulation does not provide a reliable basis for modelling SWC in the given ecosystem. FlAc succeeded in May and June to reveal a significant relationship with SWC, and significant responses for Slope15 were observed during the winter month only. Higher ranges of SWC coincided with steeper slopes. This could be due to the fact that the soil properties in the low mountain ranges of Central Europe differ strongly within a small area, while those properties in turn depend on topography. For instance, different depths of organic layer depend on the topography with lower thicknesses on the steeper areas of the upper slopes. The higher range can be attributed to faster desiccation on slopes, which can be explained by slope inclination and preferential flows. The relatively deep colluvium in the valley areas is a special feature of the study area, representing an indication of intensive agricultural use in the study area in former days (Langewitz et al., 2021). However, the occurrence of thick organic layers in valleys obscure the interrelation between soil properties and topography, as the organic topsoil layers feature higher thickness as compared to plateau and slope sites, depending on the upper slope and the slope morphology.

The different settings of DTW accounting for drier and wetter conditions failed in explaining spatial and temporal variations of SWC. In theory, DTW maps with a high flow initiation area (as DTW4) are designed to reflect conditions of low overall SWC (Jones and Arp, 2019). This would lead to a temporal shift of best scores reached. While indices as DTW4 should have best performance during dry periods, DTW0.25 or DTW1 should dominate in periods with high moisture levels. In fact, correlation coefficient for DTW during dry month turned negative, but was weak and non-significant. During winter months, the correlation between DTW0.25 and SWC showed positive associations, contrary to expectations. These findings are in line with earlier work done in deciduous forests of central Germany: weak but significant correlations were observed between DTW and SWC (Schönauer et al., 2021b) on measuring transects positioned perpendicularly to DTW channels, yet this selection of measuring sites might have favoured the performance in predicting SWC. In a temperate forest on a *Cambisol* over limestone in Lower Saxony, Germany, DTW values were compared to 1620 systematically collected SWC measurements across an area of 252 ha – although the correlation turned out to be significant, the performance was poor, with an R^2 of 0.022 (Winkler, 2021). A similar procedure was facilitated in a mixed stand, stocking on *Cambisol* based on a silicate bedrock, where gravimetric and volumetric SWC were compared to different scenarios of DTW, but no dependency between both could be established (Schönauer et al., 2021a).

In boreal forests of Fenno-Scandinavian region and Canada, however, the variability of SWC or spatial extent of wet areas could be modelled using topographic indices with high accuracy (Campbell et al., 2013; Larson et al., 2022; White et al., 2012). This can be attributed to the fact that the soil development of the glacial series in Fennoscandia started at the same time and with same initial conditions, thus resulted in uniform soil properties over large areas with similar thickness of humus accumulation on sandy or peaty soils. The soils in Scandinavia are generally younger than those in Central Europe. In Scandinavia, glaciation stripped the land down to the bedrock, significantly delaying soil formation. In contrast, the soil in the study area have remained undisturbed for thousands to tens of thousands of years in a milder climate, enabling them to persist and mature to a greater extent. The generally lower rootable volume in younger and shallower soils also contributes to a more uniform soil water content across the landscape, as the different rooting depths represent a large uncertainty factor that cannot be easily derived from aboveground biomass or vegetation types (Blume-Werry et al., 2023; Snow et al., 2024). Apart from this, the low coefficient of determination (R^2= 0.01) suggests that other parameters play a greater role in the spatial variability and that soil properties also differ independently of the topography within the study area, as indicated from 12 local soil profiles across the study site (Diederichs, 2018). The palaeorelief of the periglacially overprinted area could play a particular role here. The different thicknesses of these layers of loose rock cover or Loess deposits determine the soil formation above them and the preferential flow paths (Fischer-Bedtke et al., 2023; Pinos et al., 2023). Small depressions and cracks, which are an indicator of preferential flow paths, are not taken into account in the 1 m DEM. In addition, the soils of Central Europe's low mountain ranges have been managed for much longer as compared to boreal sites, resulting in differences in topsoil compaction (Crawford et al., 2021; Mohieddinne et al., 2023).

In this analysis, we compared variations along both axes and showed a temporal/spatial-ratio of 3.60 for the monthly data and 3.68 for the continuous data, showing the paramount dominance of temporal variations over spatial ones. Temporal variations of the daily

and monthly data were reflected accurately by retrievals from ERA5-Land (Fig. 5). Comparisons between in-situ SWC and values of SWC_{ERA}-Layer-3 resulted in an R^2 of 0.91 or 0.87, for daily or monthly data, respectively, with an RSME of 2.7 %v/v (daily data) after adjusting the SWC_{ERA} values to the SWC levels of the site. This simple adjustment, which effectively removes the overall bias, could be applied on a broad scale with minimal in-situ data requirements. As such, it holds strong potential to enhance the quality of remotely sensed estimates, facilitating their use in both scientific research and practical forestry applications. It is to say that the coarse spatial resolution of ERA5-Land estimates does not match the spatial granularity of forest stands or districts but can be considered suitable in regional-scale contexts.

Daily in-situ SWC and ST show stronger correlations with ERA5-Land Layer-3, or Level-2, respectively, compared to Layer/Level-1, which would represent the actual measuring depth of the TMS-4 loggers or manual measurements. The better performance of SWC_{ERA} from deeper layers with in-situ values measured at upper horizons has been reported already (Schönauer et al., 2024). The dominance of open lands as the primary land cover in the region (Fig. 1B) may have contributed to the superior performance of SWC_{ERA}-Layer-3, as grasslands generally display greater temporal variability in SWC of upper soil layers as compared to the more stable soil moisture in forested areas (James et al., 2003). Since the temporal variability of SWC tends to diminish with increasing soil depth (Tromp-van Meerveld and McDonnell, 2006), partly due to smaller transpiration rates (Kelliher et al., 1993), the relationship between SWC measured in ~0–7.5 cm depth is better represented using SWC_{ERA}-Layer-3 estimations as compared to the uppermost layer. For soil temperature, higher levels and variations were found on grassland as compared to forested areas (Lembrechts et al., 2022), aligning with the bias and depth-related differences of variability in ERA-Land retrievals. These findings suggests that not only the corresponding layers of ERA5-Land estimates, but also deeper layers of the ERA5-Land products can be effectively utilized for different land use covers and regions. Future studies should critically assess the most appropriate ERA5-Land level in relation to in-situ conditions and land cover heterogeneity.

In a previous study, Schönauer et al. (2024) were unable to determine whether the study area was too small to capture spatial variations, or whether temporal variations clearly dominated over spatial ones. In this work, we base our findings on a relatively large study area with an extent of 900 × 600 m, thereby enabling a more reliable assessment of spatiotemporal variations – with variations on a temporal axis clearly exceeding spatial ones. Remote sensing or reanalysis products are suitable for covering temporal changes of SWC and ST, and although information on SWC dynamics is available at finer resolutions—such as from Sentinel-1 campaign and derived estimates (Bauer-Marschallinger et al., 2019)—we chose ERA5-Land retrievals due to their strong correlation with in-situ values of SWC (Lal et al., 2022) and ST (Yilmaz, 2023). ERA5-Land retrievals have once again proven effective in estimating temporal variations of soil states and offer clear advantages over spatial indices for various practical applications. For instance, predicting forest stand trafficability to mitigate damage from heavy forestry machinery has become common practice in Northern countries. However, in Central Europe, such applications may add limited value to existing soil protection measures, as correlations between SWC and topographic indices showed to be weak. Compared to topographic maps, ERA5-Land retrievals and their ability to represent temporal variations of soil moisture and temperature shift the initially mentioned question—*where* and *when* soils are wet—to a more actionable one: *when* are soils wet, and *when* should machine operations be avoided, particularly at the scale of forest districts.

5. Conclusion

This study presents a comprehensive analysis of the spatio-temporal distribution of soil water content (SWC) in a temperate beech forest stand in central Germany. Topographic indices derived from flow accumulation were not effective in capturing the spatial variability of SWC. However, given that spatial variability was relatively minor compared to temporal fluctuations, the practical relevance of topographic modeling may be limited in similar environments. At broader scales, soil moisture dynamics along a temporal scale may play a more significant role in informing adaptive forestry practices. The ERA5-Land dataset, with its coarse spatial resolution (9 × 9 km) but high temporal resolution, proved to be a reliable source for estimating SWC and soil temperature. It offers a valuable means of bridging the gap between infrequent field measurements and continuous high-resolution modeling. By integrating field observations, the annual absolute bias of ERA5-Land estimates can be quantified and corrected, resulting in accurate representations of local site conditions.

Climate change-driven shifts in precipitation are expected to disrupt hydrological links in deciduous forests, altering SWC variability and ecosystem functioning. To enhance our understanding of both, there is an urgent need for empirical data at diverse scales, leveraging the linkage between remote sensing products and in-situ measurements, and contributing to the improvement of methods to estimate soil moisture dynamics using different sources.

CRediT authorship contribution statement

Schönauer Marian: Writing – original draft, Visualization, Supervision, Resources, Methodology, Investigation, Formal analysis, Conceptualization. **Drollinger Simon:** Writing – original draft, Supervision, Methodology, Investigation, Formal analysis, Data curation, Conceptualization. **Sauer Daniela:** Writing – review & editing, Resources, Funding acquisition. **Asabere Stephen B.:** Writing – review & editing, Validation, Investigation.

Declaration of Competing Interest

The authors declare that they have no known competing financial interests or personal relationships that could have appeared to influence the work reported in this paper.

Acknowledgements

We thank the Ministry of Science and Culture of Lower Saxony for funding the instrumentation of the study area in the frame of the program "Female professors for Lower Saxony" (FKZ 12.3–76251–99–17/15). MS was funded by the European Union under Horizon Europe (project ERA-Chair: Striving for excellence in forest ecosystem research - EXCELLENTIA, GA no. 101087262), and received financial support from the Eva Mayr-Stihl Stiftung during field work and data preparation. We are grateful to Mark-Fabian Franz for manual measurements. Many thanks to Axel Pampe (Head of the Forestry Department Reinhausen), Nils Gerke (responsible district forester), and the *Niedersächsische Landesforsten* for the support and access to the study site.

Appendix A. Supporting information

Supplementary data associated with this article can be found in the online version at doi:10.1016/j.ejrh.2025.102456.

References

Adams, H.R., Barnard, H.R., Loomis, A.K., 2014. Topography alters tree growth–climate relationships in a semi-arid forested catchment. Ecosphere 5, 1–16. https://doi.org/10.1890/ES14-00296.1.

Ågren, A., Larson, J., Paul, S.S., Laudon, H., Lidberg, W., 2021. Use of multiple LIDAR-derived digital terrain indices and machine learning for high-resolution national-scale soil moisture mapping of the Swedish forest landscape. Geoderma 404, 115280. https://doi.org/10.1016/j.geoderma.2021.115280.

Ågren, A., Lidberg, W., Strömgren, M., Ogilvie, J., Arp, P., 2014. Evaluating digital terrain indices for soil wetness mapping – a Swedish case study. Hydrol. Earth Syst. Sci. 18, 3623–3634. https://doi.org/10.5194/hess-18-3623-2014.

Awaida, A., Westervelt, J., 2020. Geographic Resources Analysis Support System (GRASS GIS).

Bartels, S.F., Caners, R.T., Ogilvie, J., White, B., Macdonald, S.E., 2018. Relating bryophyte assemblages to a remotely sensed depth-to-water index in boreal forests. Front Plant Sci. 9. https://doi.org/10.3389/fpls.2018.00858.

Bauer-Marschallinger, B., Freeman, V., Cao, S., Paulik, C., Schaufler, S., Stachl, T., Modanesi, S., Massari, C., Ciabatta, L., Brocca, L., Wagner, W., 2019. Toward global soil moisture monitoring with sentinel-1: harnessing assets and overcoming obstacles. IEEE Trans. Geosci. Remote Sens. 57, 520–539. https://doi.org/10.1109/TGRS.2018.2858004.

Berg, A., Sheffield, J., 2018. Climate change and drought: the soil moisture perspective. Curr. Clim. Change Rep. 4, 180–191. https://doi.org/10.1007/s40641-018-0095-0.

Beven, K.J., Kirkby, M.J., 1979. A physically based, variable contributing area model of basin hydrology / Un modèle à base physique de zone d'appel variable de l'hydrologie du bassin versant. Hydrol. Sci. Bull. 24, 43–69. https://doi.org/10.1080/02626667909491834.

Bivand, R., Krug, R., Lovelace, R., Neteler, M., Jeworutzki, S., Vanderhaeghe, F., 2023. rgrass: Interface Between 'GRASS' Geographical Information System and 'R': version 0.3.9.

Blume-Werry, G., Dorrepaal, E., Keuper, F., Kummu, M., Wild, B., Weedon, J.T., 2023. Arctic rooting depth distribution influences modelled carbon emissions but cannot be inferred from aboveground vegetation type. N. Phytol. 240, 502–514. https://doi.org/10.1111/nph.18998.

Campbell, D.M.H., White, B., Arp, P., 2013. Modeling and mapping soil resistance to penetration and rutting using LiDAR-derived digital elevation data. J. Soil Water Conserv. 68, 460–473. https://doi.org/10.2489/jswc.68.6.460.

Chen, Z., Mohanty, B.P., Rodriguez-Iturbe, I., 2017. Space-time modeling of soil moisture. Adv. Water Resour. 109, 343–354. https://doi.org/10.1016/j.advwatres.2017.09.009.

Copernicus Climate Change Service, 2019. ERA5-Land hourly data from 2001 to present. ECMWF; Copernicus Climate Change Service (C3S) Climate Data Store (CDS). doi:10.24381/cds.e2161bac.

Cosby, B.J., Hornberger, G.M., Clapp, R.B., Ginn, T.R., 1984. A statistical exploration of the relationships of soil moisture characteristics to the physical properties of soils. Water Resour. Res. 20, 682–690. https://doi.org/10.1029/WR020i006p00682.

Crawford, L.J., Heinse, R., Kimsey, M.J., Page-Dumroese, D.S., 2021. Soil Sustainability and Harvest Operations. Gen. Tech. Rep. RMRS. https://doi.org/10.2737/RMRS-GTR-421.

De Oliveira, V.A., Rodrigues, A.F., Morais, M.A.V., Terra, M.D., Guo, L., De Mello, C.R., 2021. Spatiotemporal modelling of soil moisture in an Atlantic forest through machine learning algorithms. Eur. J. Soil Sci. 72, 1969–1987. https://doi.org/10.1111/ejss.13123.

Diederichs, J., 2018. Einfluss von Exposition und Kronenüberdeckung auf den Bodenwasserhaushalt in einem Buchenwald (master thesis). University of Göttingen, Göttingen.

Drollinger, S., Dietze, M., Seidel, D., Schwindt, D., Birk, J.J., Sauer, D., 2025. Recent changes in rainfall patterns alter precipitation partitioning in European beech forest. Environ. Res. Commun. 7, 031004. https://doi.org/10.1088/2515-7620/adbba4.

Evans, J.S., Murphy, M.A., 2023. spatialEco.

Feldman, A.F., Feng, X., Felton, A.J., Konings, A.G., Knapp, A.K., Biederman, J.A., Poulter, B., 2024. Plant responses to changing rainfall frequency and intensity. Nat. Rev. Earth Environ. 5, 276–294. https://doi.org/10.1038/s43017-024-00534-0.

Finnish Meteorological Institute, 2023. Harvester Seasons [WWW Document]. URL ⟨https://harvesterseasons.com/HarvesterSeasons_Description2pager_v2.pdf⟩.

Fischer-Bedtke, C., Metzger, J.C., Demir, G., Wutzler, T., Hildebrandt, A., 2023. Throughfall spatial patterns translate into spatial patterns of soil moisture dynamics – empirical evidence. Hydrol. Earth Syst. Sci. 27, 2899–2918. https://doi.org/10.5194/hess-27-2899-2023.

Fowler, H.J., Lenderink, G., Prein, A.F., Westra, S., Allan, R.P., Ban, N., Barbero, R., Berg, P., Blenkinsop, S., Do, H.X., Guerreiro, S., Haerter, J.O., Kendon, E.J., Lewis, E., Schaer, C., Sharma, A., Villarini, G., Wasko, C., Zhang, X., 2021. Anthropogenic intensification of short-duration rainfall extremes. Nat. Rev. Earth Environ. 2, 107–122. https://doi.org/10.1038/s43017-020-00128-6.

Grayson, R.B., Western, A.W., Chiew, F.H.S., Blöschl, G., 1997. Preferred states in spatial soil moisture patterns: Local and nonlocal controls. Water Resour. Res. 33, 2897–2908. https://doi.org/10.1029/97WR02174.

Green, J.K., Seneviratne, S.I., Berg, A.M., Findell, K.L., Hagemann, S., Lawrence, D.M., Gentine, P., 2019. Large influence of soil moisture on long-term terrestrial carbon uptake. Nature 565, 476–479. https://doi.org/10.1038/s41586-018-0848-x.

Greiser, C., Hederová, L., Vico, G., Wild, J., Macek, M., Kopecký, M., 2024. Higher soil moisture increases microclimate temperature buffering in temperate broadleaf forests. Agric. For. Meteorol. 345, 109828. https://doi.org/10.1016/j.agrformet.2023.109828.

Greve, P., Kahil, T., Mochizuki, J., Schinko, T., Satoh, Y., Burek, P., Fischer, G., Tramberend, S., Burtscher, R., Langan, S., Wada, Y., 2018. Global assessment of water challenges under uncertainty in water scarcity projections. Nat. Sustain 1, 486–494. https://doi.org/10.1038/s41893-018-0134-9.

Hoffmann, S., Schönauer, M., Heppelmann, J., Asikainen, A., Cacot, E., Eberhard, B., Hasenauer, H., Ivanovs, J., Jaeger, D., Lazdins, A., Mohtashami, S., Moskalik, T., Nordfjell, T., Stereńczak, K., Talbot, B., Uusitalo, J., Vuillermoz, M., Astrup, R., 2022. Trafficability prediction using depth-to-water maps: the status of application in northern and Central European forestry. Curr. For. Rep. 338, 124. https://doi.org/10.1007/s40725-021-00153-8.

Hufkens, K., Stauffer, R., Campitelli, E., 2019. ecmwfr: Programmatic interface to the two European Centre for Medium-Range Weather Forecasts API services. doi:10.5281/zenodo.2647531.

James, S.E., Pärtel, M., Wilson, S.D., Peltzer, D.A., 2003. Temporal heterogeneity of soil moisture in grassland and forest. J. Ecol. 91, 234239.

Jones, M.-F., Arp, P., 2019. Soil trafficability forecasting. Open J. For. 9 296–322. https://doi.org/10.4236/ojf.2019.94017.

Kelliher, F.M., Leuning, R., Schulze, E.D., 1993. Evaporation and canopy characteristics of coniferous forests and grasslands. Oecologia 95, 153–163. https://doi.org/10.1007/BF00323485.

Konapala, G., Mishra, A.K., Wada, Y., Mann, M.E., 2020. Climate change will affect global water availability through compounding changes in seasonal precipitation and evaporation. Nat. Commun. 11, 3044. https://doi.org/10.1038/s41467-020-16757-w.

Lal, P., Singh, G., Das, N.N., Colliander, A., Entekhabi, D., 2022. Assessment of ERA5-Land volumetric soil water layer product using in situ and SMAP soil moisture observations. IEEE Geosci. Remote Sens. Lett. 19, 1–5. https://doi.org/10.1109/LGRS.2022.3223985.

Langewitz, T., Wiedner, K., Polifka, S., Eckmeier, E., 2021. Pedological properties related to formation and functions of ancient ridge and furrow cultivation in Central and Northern Germany. CATENA 198, 105049. https://doi.org/10.1016/j.catena.2020.105049.

Larson, J., Lidberg, W., Ågren, A.M., Laudon, H., 2022. Predicting soil moisture conditions across a heterogeneous boreal catchment using terrain indices. Hydrol. Earth Syst. Sci. 26, 4837–4851. https://doi.org/10.5194/hess-26-4837-2022.

Latterini, F., Venanzi, R., Papa, I., Đuka, A., Picchio, R., 2024. A meta-analysis to evaluate the reliability of depth-to-water maps in predicting areas particularly sensitive to machinery-induced soil disturbance. Croat. J. For. Eng. 45, 433–444. https://doi.org/10.5552/crojfe.2024.2559.

Lembrechts, J.J., Van Den Hoogen, J., Aalto, J., Ashcroft, M.B., De Frenne, P., Kemppinen, J., Kopecký, M., Luoto, M., Maclean, I.M.D., Crowther, T.W., Bailey, J.J., Haesen, S., Klinges, D.H., Niittynen, P., Scheffers, B.R., Van Meerbeek, K., Aartsma, P., Abdalaze, O., Abedi, M., Aerts, R., Ahmadian, N., Ahrends, A., Alatalo, J. M., Alexander, J.M., Allonsius, C.N., Altman, J., Ammann, C., Andres, C., Andrews, C., Ardö, J., Arriga, N., Arzac, A., Aschero, V., Assis, R.L., Assmann, J.J., Bader, M.Y., Bahalkeh, K., Barančok, P., Barrio, I.C., Barros, A., Barthel, M., Basham, E.W., Bauters, M., Bazzichetto, M., Marchesini, L.B., Bell, M.C., Benavides, J. C., Benito Alonso, J.L., Berauer, B.J., Bjerke, J.W., Björk, R.G., Björkman, M.P., Björnsdóttir, K., Blonder, B., Boeckx, P., Boike, J., Bokhorst, S., Brum, B.N.S., Brůna, J., Buchmann, N., Buysse, P., Camargo, J.L., Campoe, O.C., Candan, O., Canessa, R., Cannone, N., Carbognani, M., Carnicer, J., Casanova-Katny, A., Cesarz, S., Chojnicki, B., Choler, P., Chown, S.L., Cifuentes, E.F., Čiliak, M., Contador, T., Convey, P., Cooper, E.J., Cremonese, E., Curasi, S.R., Curtis, R., Cutini, M., Dahlberg, C.J., Daskalova, G.N., De Pablo, M.A., Della Chiesa, S., Dengler, J., Deronde, B., Descombes, P., Di Cecco, V., Di Musciano, M., Dick, J., Dimarco, R.D., Dolezal, J., Dorrepaal, E., Dušek, J., Eisenhauer, N., Eklundh, L., Erickson, T.E., Erschbamer, B., Eugster, W., Ewers, R.M., Exton, D.A., Fanin, N., Fazlioglu, F., Feigenwinter, I., Fenu, G., Ferlian, O., Fernández Calzado, M.R., Fernández-Pascual, E., Finckh, M., Higgens, R.F., Forte, T.G.W., Freeman, E.C., Frei, E.R., Fuentes-Lillo, E., García, R.A., García, M.B., Géron, C., Gharun, M., Ghosn, D., Gigauri, K., Gobin, A., Goded, I., Goeckede, M., Gottschall, F., Goulding, K., Govaert, S., Graae, B.J., Greenwood, S., Greiser, C., Grelle, A., Guénard, B., Guglielmin, M., Guillemot, J., Haase, P., Haider, S., Halbritter, A.H., Hamid, M., Hammerle, A., Hampe, A., Haugum, S.V., Hederová, L., Heinesch, B., Helfter, C., Hepenstrick, D., Herberich, M., Herbst, M., Hermanutz, L., Hik, D.S., Hoffrén, R., Homeier, J., Hörtnagl, L., Høye, T.T., Hrbacek, F., Hylander, K., Iwata, H., Jackowicz-Korczynski, M.A., Jactel, H., Järveoja, J., Jastrzębowski, S., Jentsch, A., Jiménez, J.J., Jónsdóttir, I.S., Jucker, T., Jump, A.S., Juszczak, R., Kanka, R., Kašpar, V., Kazakis, G., Kelly, J., Khuroo, A.A., Klemedtsson, L., Klisz, M., Kljun, N., Knohl, A., Kobler, J., Kollár, J., Kotowska, M.M., Kovács, B., Kreyling, J., Lamprecht, A., Lang, S.I., Larson, C., Larson, K., Laska, K., Le Maire, G., Leihy, R.I., Lens, L., Liljebladh, B., Lohila, A., Lorite, J., Loubet, B., Lynn, J., Macek, M., Mackenzie, R., Magliulo, E., Maier, R., Malfasi, F., Máliš, F., Man, M., Manca, G., Manco, A., Manise, T., Manolaki, P., Marciniak, F., Matula, R., Mazzolari, A.C., Medinets, S., Medinets, V., Meeussen, C., Merinero, S., Mesquita, R.D.C.G., Meusburger, K., Meysman, F.J.R., Michaletz, S.T., Milbau, A., Moiseev, D., Moiseev, P., Mondoni, A., Monfries, R., Montagnani, L., Moriana-Armendariz, M., Morra Di Cella, U., Mörsdorf, M., Mosedale, J.R., Muffler, L., Muñoz-Rojas, M., Myers, J.A., Myers-Smith, I.H., Nagy, L., Nardino, M., Naujokaitis-Lewis, I., Newling, E., Nicklas, L., Niedrist, G., Niessner, A., Nilsson, M.B., Normand, S., Nosetto, M.D., Nouvellon, Y., Nuñez, M.A., Ogaya, R., Ogée, J., Okello, J., Olejnik, J., Olesen, J.E., Opedal, Ø.H., Orsenigo, S., Palaj, A., Pampuch, T., Panov, A.V., Pärtel, M., Pastor, A., Pauchard, A., Pauli, H., Pavelka, M., Pearse, W.D., Peichl, M., Pellissier, L., Penczykowski, R.M., Penuelas, J., Petit Bon, M., Petraglia, A., Phartyal, S.S., Phoenix, G.K., Pio, C., Pitacco, A., Pitteloud, C., Plichta, R., Porro, F., Portillo-Estrada, M., Poulenard, J., Poyatos, R., Prokushkin, A.S., Puchalka, R., Puşcaş, M., Radujković, D., Randall, K., Ratier Backes, A., Remmele, S., Remmers, W., Renault, D., Risch, A.C., Rixen, C., Robinson, S.A., Robroek, B.J.M., Rocha, A.V., Rossi, C., Rossi, G., Roupsard, O., Rubtsov, A.V., Saccone, P., Sagot, C., Sallo Bravo, J., Santos, C.C., Sarneel, J.M., Scharnweber, T., Schmeddes, J., Schmidt, M., Scholten, T., Schuchardt, M., Schwartz, N., Scott, T., Seeber, J., Segalin De Andrade, A.C., Seipel, T., Semenchuk, P., Senior, R.A., Serra-Diaz, J.M., Sewerniak, P., Shekhar, A., Sidenko, N.V., Siebicke, L., Siegwart Collier, L., Simpson, E., Siqueira, D.P., Sitková, Z., Six, J., Smiljanic, M., Smith, S.W., Smith-Tripp, S., Somers, B., Sørensen, M.V., Souza, J.J.L.L., Souza, B.I., Souza Dias, A., Spasojevic, M.J., Speed, J.D.M., Spicher, F., Stanisci, A., Steinbauer, K., Steinbrecher, R., Steinwandter, M., Stemkovski, M., Stephan, J.G., Stiegler, C., Stoll, S., Svátek, M., Svoboda, M., Tagesson, T., Tanentzap, A.J., Tanneberger, F., Theurillat, J., Thomas, H.J.D., Thomas, A.D., Tielbörger, K., Tomaselli, M., Treier, U.A., Trouillier, M., Turtureanu, P.D., Tutton, R., Tyystjärvi, V.A., Ueyama, M., Ujházy, K., Ujházyová, M., Uogintas, D., Urban, A.V., Urban, J., Urbaniak, M., Ursu, T., Vaccari, F.P., Van De Vondel, S., Van Den Brink, L., Van Geel, M., Vandvik, V., Vangansbeke, P., Varlagin, A., Veen, G.F., Veenendaal, E., Venn, S.E., Verbeeck, H., Verbrugggen, E., Verheijen, F.G.A., Villar, L., Vitale, L., Vittoz, P., Vives-Ingla, M., Von Oppen, J., Walz, J., Wang, R., Wang, Y., Way, R.G., Wedegärtner, R.E.M., Weigel, R., Wild, J., Wilkinson, M., Wilmking, M., Wingate, L., Winkler, M., Wipf, S., Wohlfahrt, G., Xenakis, G., Yang, Y., Yu, Z., Yu, K., Zellweger, F., Zhang, J., Zhang, Z., Zhao, P., Zieblińska, K., Zimmermann, R., Zong, S., Zyryanov, V.I., Nijs, I., Lenoir, J., 2022. Global maps of soil temperature. Glob. Change Biol. 28, 3110–3144. https://doi.org/10.1111/gcb.16060.

Li, W., Migliavacca, M., Forkel, M., Denissen, J.M.C., Reichstein, M., Yang, H., Duveiller, G., Weber, U., Orth, R., 2022. Widespread increasing vegetation sensitivity to soil moisture. Nat. Commun. 13, 3959. https://doi.org/10.1038/s41467-022-31667-9.

Liang, J., Liu, Q., Zhang, H., Li, Xiaodong, Qian, Z., Lei, M., Li, Xin, Peng, Y., Li, S., Zeng, G., 2020. Interactive effects of climate variability and human activities on blue and green water scarcity in rapidly developing watershed. J. Clean. Prod. 265, 121834. https://doi.org/10.1016/j.jclepro.2020.121834.

Liu, Y., Jing, W., Wang, Q., Xia, X., 2020. Generating high-resolution daily soil moisture by using spatial downscaling techniques: a comparison of six machine learning algorithms. Adv. Water Resour. 141, 103601. https://doi.org/10.1016/j.advwatres.2020.103601.

Martinez, G., Pachepsky, Y.A., Vereecken, H., Hardelauf, H., Herbst, M., Vanderlinden, K., 2013. Modeling local control effects on the temporal stability of soil water content. J. Hydrol. 481, 106–118. https://doi.org/10.1016/j.jhydrol.2012.12.024.

Mohieddinne, H., Brasseur, B., Gallet-Moron, E., Lenoir, J., Spicher, F., Kobaissi, A., Horen, H., 2023. Assessment of soil compaction and rutting in managed forests through an airborne LiDAR technique. Land Degrad. Dev. 34, 1558–1569. https://doi.org/10.1002/ldr.4553.

mundialis GmbH & Co. KG, 2025. Landcover classification map of Germany 2021 based on Sentinel-2 data.

Muñoz-Sabater, J., Dutra, E., Agustí-Panareda, A., Albergel, C., Arduini, G., Balsamo, G., Boussetta, S., Choulga, M., Harrigan, S., Hersbach, H., Martens, B., Miralles, D.G., Piles, M., Rodríguez-Fernández, N.J., Zsoter, E., Buontempo, C., Thépaut, J.-N., 2021. ERA5-Land: a state-of-the-art global reanalysis dataset for land applications. Earth Syst. Sci. Data 13, 4349–4383. https://doi.org/10.5194/essd-13-4349-2021.

Murphy, P.N.C., Ogilvie, J., Arp, P., 2009. Topographic modelling of soil moisture conditions: a comparison and verification of two models. Eur. J. Soil Sci. 60, 94–109. https://doi.org/10.1111/j.1365-2389.2008.01094.x.

Murphy, P.N.C., Ogilvie, J., Connor, K., Arp, P., 2007. Mapping wetlands: a comparison of two different approaches for New Brunswick, Canada. WETLANDS 27, 846–854. https://doi.org/10.1672/0277-5212(2007)27[846:MWACOT]2.0.CO;2.

Murphy, P.N.C., Ogilvie, J., Meng, F.-R., White, B., Bhatti, J.S., Arp, P., 2011. Modelling and mapping topographic variations in forest soils at high resolution: a case study. Ecol. Model. 222, 2314–2332. https://doi.org/10.1016/j.ecolmodel.2011.01.003.

Nguyen, T.T., Ngo, H.H., Guo, W., Chang, S.W., Nguyen, D.D., Nguyen, C.T., Zhang, J., Liang, S., Bui, X.T., Hoang, N.B., 2022. A low-cost approach for soil moisture prediction using multi-sensor data and machine learning algorithm. Sci. Total Environ. 833, 155066. https://doi.org/10.1016/j.scitotenv.2022.155066.

Nketia, K.A., Asabere, S.B., Ramcharan, A., Herbold, S., Erasmi, S., Sauer, D., 2022. Spatio-temporal mapping of soil water storage in a semi-arid landscape of northern Ghana – a multi-tasked ensemble machine-learning approach. Geoderma 410, 115691. https://doi.org/10.1016/j.geoderma.2021.115691.

O, S., Orth, R., 2021. Global soil moisture data derived through machine learning trained with in-situ measurements. Sci Data 8, 170. https://doi.org/10.1038/s41597-021-00964-1.

Pendergrass, A.G., Knutti, R., Lehner, F., Deser, C., Sanderson, B.M., 2017. Precipitation variability increases in a warmer climate. Sci. Rep. 7, 17966. https://doi.org/10.1038/s41598-017-17966-y.

Peng, J., Albergel, C., Balenzano, A., Brocca, L., Cartus, O., Cosh, M.H., Crow, W.T., Dabrowska-Zielinska, K., Dadson, S., Davidson, M.W.J., De Rosnay, P., Dorigo, W., Gruber, A., Hagemann, S., Hirschi, M., Kerr, Y.H., Lovergine, F., Mahecha, M.D., Marzahn, P., Mattia, F., Musial, J.P., Preuschmann, S., Reichle, R.H., Satalino, G., Silgram, M., Van Bodegom, P.M., Verhoest, N.E.C., Wagner, W., Walker, J.P., Wegmüller, U., Loew, A., 2021. A roadmap for high-resolution satellite soil moisture applications – confronting product characteristics with user requirements. Remote Sens. Environ. 252, 112162. https://doi.org/10.1016/j.rse.2020.112162.

Pinos, J., Flury, M., Latron, J., Llorens, P., 2023. Routing stemflow water through the soil via preferential flow: a dual-labelling approach with artificial tracers. Hydrol. Earth Syst. Sci. 27, 2865–2881. https://doi.org/10.5194/hess-27-2865-2023.

R Core Team, 2023. R: A Language and Environment for Statistical Computing. R Foundation for Statistical Computing, Vienna. https://www.R-project.org/.

Rahmati, M., Amelung, W., Brogi, C., Dari, J., Flammini, A., Bogena, H., Brocca, L., Chen, H., Groh, J., Koster, R.D., McColl, K.A., Montzka, C., Moradi, S., Rahi, A., Sharghi, S., F., Vereecken, H., 2024. Soil moisture memory: state-of-the-art and the way forward. Rev. Geophys. 62, e2023RG000828. https://doi.org/10.1029/2023RG000828.

S.U, S.L., Singh, D.N., Shojaei Baghini, M., 2014. A critical review of soil moisture measurement. Measurement 54, 92–105. https://doi.org/10.1016/j.measurement.2014.04.007.

Scharnagl, B., Vrugt, J.A., Vereecken, H., Herbst, M., 2011. Inverse modelling of in situ soil water dynamics: investigating the effect of different prior distributions of the soil hydraulic parameters. Hydrol. Earth Syst. Sci. 15, 3043–3059. https://doi.org/10.5194/hess-15-3043-2011.

Schönauer, M., Ågren, A.M., Katzensteiner, K., Hartsch, F., Arp, P., Drollinger, S., Jaeger, D., 2024. Soil moisture modeling with ERA5-Land retrievals, topographic indices, and in situ measurements and its use for predicting ruts. Hydrol. Earth Syst. Sci. 28, 2617–2633. https://doi.org/10.5194/hess-28-2617-2024.

Schönauer, M., Hoffmann, S., Maack, J., Jansen, M., Jaeger, D., 2021a. Comparison of selected terramechanical test procedures and cartographic indices to predict rutting caused by machine traffic during a cut-to-length thinning operation. Forests 12, 113. https://doi.org/10.3390/f12020113.

Schönauer, M., Prinz, R., Väätäinen, K., Astrup, R., Pszenny, D., Lindeman, H., Jaeger, D., 2022. Spatio-temporal prediction of soil moisture using soil maps, topographic indices and SMAP retrievals. Int. J. Appl. Earth Obs. Geoinf. 108, 102730. https://doi.org/10.1016/j.jag.2022.102730.

Schönauer, M., Väätäinen, K., Prinz, R., Lindeman, H., Pszenny, D., Jansen, M., Maack, J., Talbot, B., Astrup, R., Jaeger, D., 2021b. Spatio-temporal prediction of soil moisture and soil strength by depth-to-water maps. Int. J. Appl. Earth Obs. Geoinf. 105, 102614. https://doi.org/10.1016/j.jag.2021.102614.

Schönauer, M., Maack, J. 2021. R-code for calculating depth-to-water (DTW) maps using GRASS GIS (Version v1). doi:10.5281/zenodo.5638518.

Schyns, J.F., Hoekstra, A.Y., Booij, M.J., 2015. Review and classification of indicators of green water availability and scarcity. Hydrol. Earth Syst. Sci. 19, 4581–4608. https://doi.org/10.5194/hess-19-4581-2015.

Snow, D., White, E., Afriyie, N.A.O., Arp, P.A., 2024. Modelling and mapping likely soil rutting occurrences across forested areas. JGIS 16, 397–417. https://doi.org/10.4236/jgis.2024.166023.

Sørensen, R., Zinko, U., Seibert, J., 2006. On the calculation of the topographic wetness index: evaluation of different methods based on field observations. Hydrol. Earth Syst. Sci. 10, 101–112. https://doi.org/10.5194/hess-10-101-2006.

Te Wierik, S.A., Gupta, J., Cammeraat, E.L.H., Artzy-Randrup, Y.A., 2020. The need for green and atmospheric water governance. WIREs Water 7, e1406. https://doi.org/10.1002/wat2.1406.

TOMST s.r.o., n.d. TMS3Calibr, Conversion tool for raw moisture signal (~500-3600) into volumetric soil moisture (0-100% vol.).

Tromp-van Meerveld, H.J., McDonnell, J.J., 2006. On the interrelations between topography, soil depth, soil moisture, transpiration rates and species distribution at the hillslope scale. Adv. Water Resour. 29, 293–310. https://doi.org/10.1016/j.advwatres.2005.02.016.

Vereecken, H., Amelung, W., Bauke, S.L., Bogena, H., Brüggemann, N., Montzka, C., Vanderborght, J., Bechtold, M., Blöschl, G., Carminati, A., Javaux, M., Konings, A. G., Kusche, J., Neuweiler, I., Or, D., Steele-Dunne, S., Verhoef, A., Young, M., Zhang, Y., 2022. Soil hydrology in the Earth system. Nat. Rev. Earth Environ. 3, 573–587. https://doi.org/10.1038/s43017-022-00324-6.

Vereecken, H., Huisman, J.A., Pachepsky, Y., Montzka, C., van der Kruk, J., Bogena, H., Weihermüller, L., Herbst, M., Martinez, G., Vanderborght, J., 2014. On the spatio-temporal dynamics of soil moisture at the field scale. J. Hydrol. 516, 76–96. https://doi.org/10.1016/j.jhydrol.2013.11.061.

Vicente-Serrano, S.M., McVicar, T.R., Miralles, D.G., Yang, Y., Tomas-Burguera, M., 2020. Unraveling the influence of atmospheric evaporative demand on drought and its response to climate change. WIREs Clim. Change 11, e632. https://doi.org/10.1002/wcc.632.

Western, A.W., Blöschl, G., 1999. On the spatial scaling of soil moisture. J. Hydrol. 217, 203–224. https://doi.org/10.1016/S0022-1694(98)00232-7.

White, B., Ogilvie, J., Campbell, D.M.H., Hiltz, D., Gauthier, B., Chisholm, H.K., Wen, H.K., Murphy, P.N.C., Arp, P., 2012. Using the cartographic depth-to-water index to locate small streams and associated wet areas across landscapes. Can. Water Resour. J. 37, 333–347. https://doi.org/10.4296/cwrj2011-909.

Wild, J., Kopecký, M., Macek, M., Šanda, M., Jankovec, J., Haase, T., 2019. Climate at ecologically relevant scales: A new temperature and soil moisture logger for long-term microclimate measurement. Agric. For. Meteorol. 268, 40–47. https://doi.org/10.1016/j.agrformet.2018.12.018.

Winkler, M., 2021. Analysis of the skid train grid in Groner Holz (Report for course 'Development of a Forest Region' in programme "Master Tropical and International Forestry (TIF)"). University of Goettingne, Göttingen, Göttingen, Germany.

Wood, R.R., Ludwig, R., 2020. Analyzing internal variability and forced response of subdaily and daily extreme precipitation over Europe. Geophys. Res. Lett. 47, e2020GL089300. https://doi.org/10.1029/2020GL089300.

Yilmaz, M., 2023. Accuracy assessment of temperature trends from ERA5 and ERA5-Land. Sci. Total Environ. 856, 159182. https://doi.org/10.1016/j.scitotenv.2022.159182.

Zhou, S., Williams, A.P., Lintner, B.R., Berg, A.M., Zhang, Y., Keenan, T.F., Cook, B.I., Hagemann, S., Seneviratne, S.I., Gentine, P., 2021. Soil moisture–atmosphere feedbacks mitigate declining water availability in drylands. Nat. Clim. Chang 11, 38–44. https://doi.org/10.1038/s41558-020-00945-z.